International Journal of Engineering Research and Development
e- ISSN: 2278-067X, p-ISSN: 2278-800X, www.ijerd.com
Volume 22, Issue 7 (July 2026), PP 141-158

Comparative analysis of PI and GAO-Based MPPT Controllers in Fuel-Cell-Battery Hybrid Electric Vehicles

Gali Naresh[1], Dr. D VenkataBrahmaNaidu[2] ,
Dr R. Thamizhselvan[3], Battula Surya Teja[4]

[1,4] M.tech Student, Dept. of Electrical and Electronics Engineering, S.V. University ,Tirupati-517502

[2] Research Supervisor, Dept. of Electrical and Electronics Engineering, S.V. University ,Tirupati-517502

Associate Professor, Department of Electrical Engineering, Annamalai University, Chidambaram, T.N- 608002

ABSTRACT: *The increasing demand for clean and efficient transportation has accelerated the development of Fuel Cell-Battery Hybrid Electric Vehicles (FC-BHEVs). Efficient energy management and Maximum Power Point Tracking (MPPT) are essential to maximize fuel cell output and ensure stable vehicle operation under varying load conditions. This thesis presents the design and control of a Maximum Power Point Tracking system for a Fuel Cell-Battery Hybrid Electric Vehicle using Perturb and Observe (P&O) and Incremental Conductance (INC) MPPT techniques integrated with a conventional Proportional-Integral (PI) controller and a Gazelle Optimization Algorithm (GAO)-based controller. The proposed system is modelled and simulated in MATLAB/Simulink to evaluate its dynamic and steady-state performance. The controller performance is assessed using fuel cell voltage, fuel cell current, DC-link voltage, and motor speed responses. Simulation results demonstrate that the GAO-based controller significantly improves system performance compared to the conventional PI controller. The GAO controller achieves a minimum fuel cell voltage settling time of 0.1011 s and reduces the current overshoot from 10.040% to 1.097%. The GAO–INC configuration provides the best DC-link voltage regulation with a peak voltage of 517.648V, overshoot of 8.890%, and ripple of 0.297%. Additionally, the motor speed reaches steady state in 21.6416s, indicating improved dynamic response and enhanced drive stability. The comparative analysis confirms that the GAO integrated with the INC-MPPT algorithm provides superior transient and steady-state performance by reducing settling time, overshoot, and ripple while improving voltage regulation and speed stability. The proposed control strategy enhances energy utilization, system reliability, and overall efficiency, making it a promising solution for fuel cell electric vehicles, hybrid electric vehicles, and advanced renewable energy-based transportation systems.*

Keywords: *Fuel Cell-Battery Hybrid Electric Vehicle, MPPT, Gazelle Optimization Algorithm, PI Controller, P&O, Incremental Conductance, MATLAB/Simulink.*

Date of Submission: 09-07-2026 Date of acceptance: 20-07-2026

I. INTRODUCTION

The rapid growth of the transportation sector has significantly increased global energy consumption and environmental pollution due to the extensive use of fossil fuels. Conventional internal combustion engine (ICE) vehicles emit harmful greenhouse gases and pollutants that contribute to climate change and deteriorating air quality. Consequently, the automotive industry is shifting toward clean, sustainable, and energy-efficient transportation technologies. Fuel cell electric vehicles (FCEVs) overcome many of these limitations by converting the chemical energy of hydrogen directly into electrical energy through an electrochemical reaction. Fuel cells offer high energy conversion efficiency, rapid refueling, quiet operation, and environmentally friendly performance, producing only water and heat as by-products.

However, fuel cells exhibit relatively slow dynamic response during rapid load changes and are less effective in handling sudden power demands. To address these challenges, hybridizing a fuel cell with a battery energy storage system (BESS) has become an effective solution for electric vehicle applications. In a Fuel Cell–Battery Hybrid Electric Vehicle (FC-BEV), the fuel cell acts as the primary energy source, while the battery provides additional power during acceleration, absorbs regenerative braking energy, and supports the fuel cell during transient operating conditions. An important aspect of fuel cell-based hybrid systems is the efficient utilization of the fuel cell output. The electrical characteristics of a fuel cell vary with operating conditions such as load demand, hydrogen supply, and temperature.

Therefore, it is essential to operate the fuel cell at its Maximum Power Point (MPP) to maximize energy extraction and improve overall system efficiency In the proposed system, the fuel cell is interfaced with a DC–DC boost converter controlled by an MPPT algorithm to extract maximum available power. The battery energy storage system is connected to the DC bus through a bidirectional DC–DC converter, allowing it to either supply power during high-load conditions or absorb excess energy when the fuel cell output exceeds the load demand.

The entire Fuel Cell–Battery Hybrid Electric Vehicle system is modeled and simulated using the MATLAB/Simulink platform. The simulation investigates the effectiveness of the MPPT-based control strategy in improving fuel cell power extraction, maintaining DC bus voltage stability, coordinating power sharing between the fuel cell and battery, and enhancing the overall performance of the hybrid electric vehicle. Performance evaluation is carried out under varying load conditions to assess the dynamic response, power management capability, and operational efficiency of the proposed system.

The proposed MPPT-controlled fuel cell–battery hybrid architecture provides an efficient and reliable energy management solution for next-generation electric vehicles. By combining the high energy density of fuel cells with the high-power density of batteries, the system achieves improved efficiency, better transient performance, enhanced driving capability, and reduced environmental impact. The outcomes of this work contribute to the development of advanced hybrid electric vehicle technologies capable of meeting future transportation and sustainability requirements. Hydrogen, with its significant potential, serves as a versatile and efficient means to store and distribute clean energy across several economic sectors such as transportation (Electric vehicles (EV)) at different scales. Designing fuel cell (FC) systems with battery energy storage systems (BESS) creates a hybrid system that is efficient and has increased range. As such, several energy management strategies (EMS) to optimize the power sharing between the FC and the battery have been implemented. In [1], the authors have used a non-linear model predictive (MPC) method for real time energy management.

Similarly, model-based reinforcement learning and model-free reinforcement learning techniques were used for developing the EMS for the FC - battery EV (FCBEV) in [2]. In addition, an ultra-capacitor was added to the FCBEV and the impact of the EMS to find the best trade-off between the number of startup/shut down cycles and the hydrogen consumption in [3]. The EMS investigated included fixed set point operation, charge-balancing and predictive energy management. A fuzzy logic control approach was used in [4] to implement the controller for a FCBEV. A power sharing algorithm that operates the FC at its minimum operation set point to avoid multiple start up/shutdown sequences and using the battery power for additional power is proposed in [5]. The algorithm is used to control a dual input inverter that drives the electrical motor.

A hierarchical rule based and cost optimization algorithm is used to compare the performance of a single stack FC and a multiple stack FC in [6]. An overview of integrating FC with BESS for marine vessels has been presented in [8]. Additional power sharing schemes for the EMS have also been researched in [8] and [9]. In order to integrate the FC with the electric powertrain, A DC/DC boost converter is typically necessary to increase the voltage of the FC to those required by the system. During operation, it is important to control the FC power output. To achieve this, a controller is required that can govern the duty cycle of the DC/DC converter and control the power flow between the load and the FC. Among the several control techniques implemented, the Maximum Power Point Tracking (MPPT) method is one of the most commonly used. According to [10], there are four types of MPPT techniques. However, Incremental Conductance (IC) and Perturbation and Observation (P&O) are the most widely used MPPT techniques. Several authors have implemented these techniques for stationary and mobile FC applications. In [11], authors implemented the P&O algorithm to control the FC output power for a refrigeration cycle load profile.

A Fuzzy Logic Maximum Power Point Tracking (MPPT) control technique was used in [12] to sustain the operation of a FC at a specific efficiency point, considering variations in the system temperature. The authors in [13] combined the P&O MPPT method with the current reference generator to develop a FC System which includes the DC-DC Boost Converter while incremental resistance technique was used in [14] to improve the performance of the FC.

Although MPPT techniques have been widely implemented and evaluated in FC-converters systems, proving to be simple and effective, the feasibility of implementing them in an electric vehicle system under a driving profile is still not clear. Therefore, the objectives in this research study were to present the impact of a drive cycle on the performance of P&O and IC MPPT control algorithm for the FC in the FCBEV.

II. PROPOSED SYSTEM DESCRIPTION

2.1 System Model

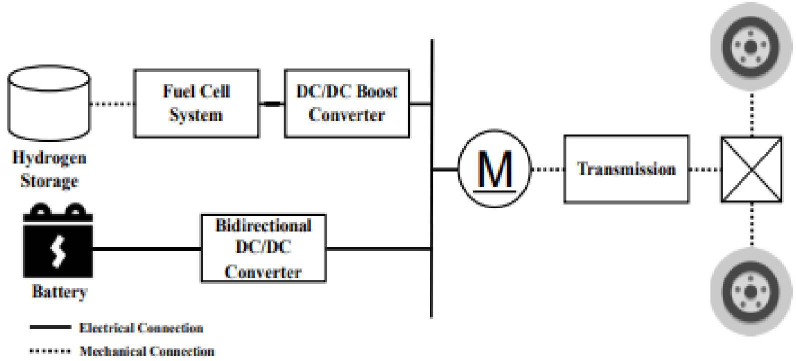

Figure 1 : System under consideration

The FC-Battery System for the EV is shown in Figure 1. The FC is connected to a DC-DC Boost converter while the battery is connected to a bidirectional converter (BDC). The BDC implements the controls for the battery charging and discharging. Both the systems are fed into a permanent magnet DC Motor (PMDC)evasion interest, such as types of species, abundance of single species, the species is local or migrant.

2.2 Driving Profile

To evaluate the performance of the proposed Maximum Power Point Tracking (MPPT) control techniques, the Worldwide Harmonised Light Vehicle Test Procedure (WLTP) driving profile was adopted as the input driving cycle as shown in Figure 2. The WLTP is an internationally recognized testing standard developed to provide realistic vehicle operating conditions by incorporating a wide range of driving speeds, acceleration, deceleration, cruising, and idling events. Compared with earlier driving cycles, the WLTP more accurately represents real-world driving behaviour and is widely used to assess the energy efficiency and dynamic performance of electric and hybrid electric vehicles.

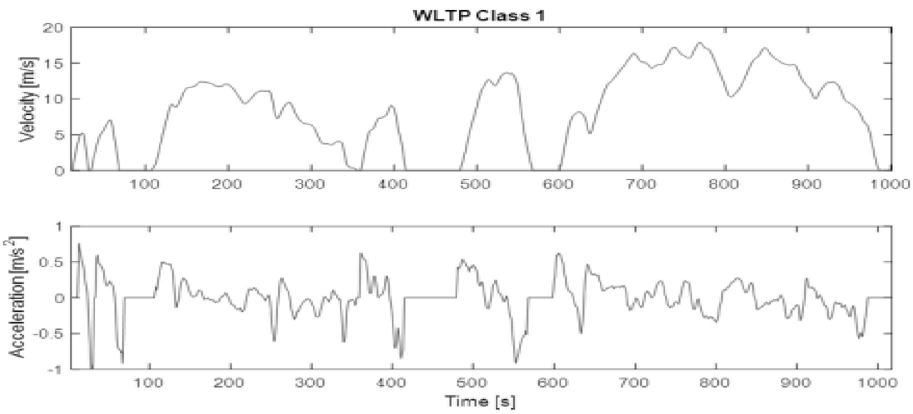

Figure 2: The driving profile used to evaluate the performance of the developed control in this study.

2.3 Battery & BDC

For preliminary simulations in this study, a BESS system with a BDC and PMDC was developed. The BESS was rated at 60 V, 400 Ah and the PMDC was a 5 HP, 480 V system, 1750 rpm. The circuit for the BDC is shown in Figure 3 below. The parameters for the BDC are shown in the given Table 1.

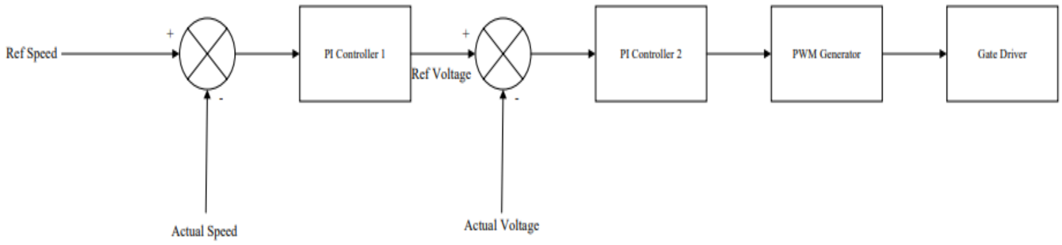

Figure 3: BDC Control System

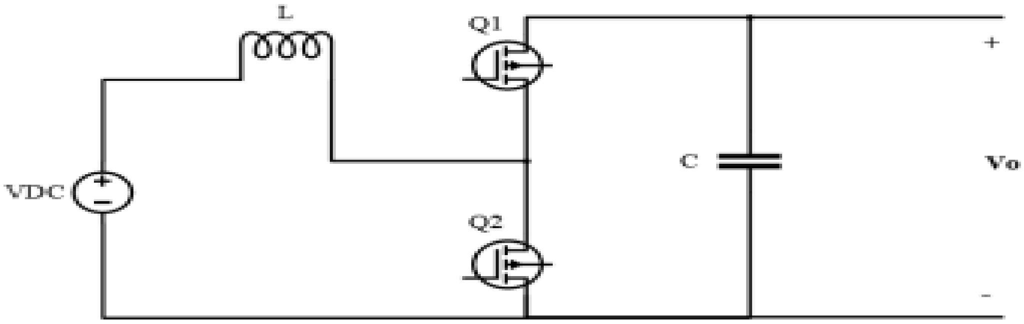

Figure 4: BDC Circuit diagram

Table 1: Bidirectional Converter Parameters

Parameter	Value
Input Voltage	60V
Output Voltage	240V
Switching Frequency	10kHz
Inductance	10μH
Capacitance	10mF

Table 2: PI Controllers Gains

Controller	Proportional Gain (Kp)	Integral Gain (Ki)
Controller 1	1	0.8
Controller 2	0.007	0.1

The control for the BDC is determined using two proportional-integral (PI) controllers as shown in Figure 4. The first PI controller is used to determine the voltage reference according the difference between the reference speed and the actual speed of the motor. The inner loop then is used to generate the switching signals for the BDC in order to control the DC bus voltage. The gains for the PI controllers are shown in Table 2.

2.4 Fuel Cell - DC Boost Converter System

For this investigation, the power curve of a commercial 45-kW FC has been derived from the datasheet [15], and the MATLAB FC Stack module has been utilized to implement the control techniques. The V-I curve was modelled according to where V_{FC} is the output voltage of the FC, Enerst is the Nerst voltage, V_{act} is the actuation losses, V_{ohmic} represents the ohmic losses and V_{conc} stands for the concentration losses, E_{cell} is the voltage across one FC, R is the ideal gas constant, T is the temperature, F is Faraday's constant, IFC is the FC current, α is the transfer coefficient, i0 is the current exchange density, R_{int} is the internal resistance of the FC. Accordingly, the FC voltage and power curves as a current function are shown in Figure 5. The converter parameters are shown in Table 3.

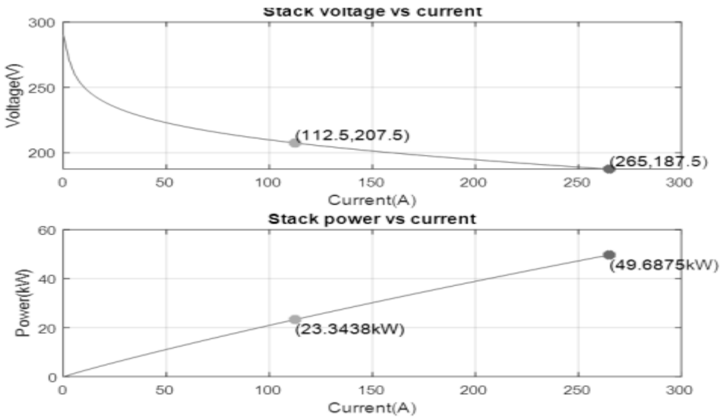

Figure 5: Characteristic curves of the 45-kW PEM Fuel Cell

Table 3: Converter Parameters

Parameter	Value
Input Voltage Range	190V–300V
Output Voltage	480V
Maximum Power	45kW
Current Ripple	25%
Voltage Ripple	5V
Switching Frequency	50kHz
Load Range	230 Ω –5.12 Ω

2.5 Maximum Power Point Tracking Algorithm

The two algorithms P&O and IC were implemented to control the Boost Converter of the FC System. Based on the actual power measurements, the MPPT algorithm will generate the voltage reference which will then be used to generate the duty cycle of the Boost Converter. The algorithm is shown in Figure 6. The IC algorithm will generate the voltage reference according to the resistance value and then the duty cycle will be generated for the boost converter switching cycle as shown in Figure 7.

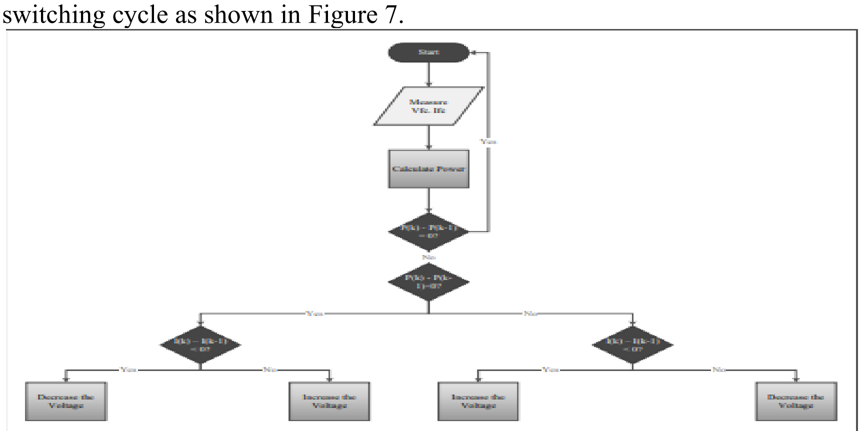

Figure 6: P&O algorithm for the Fuel Cell

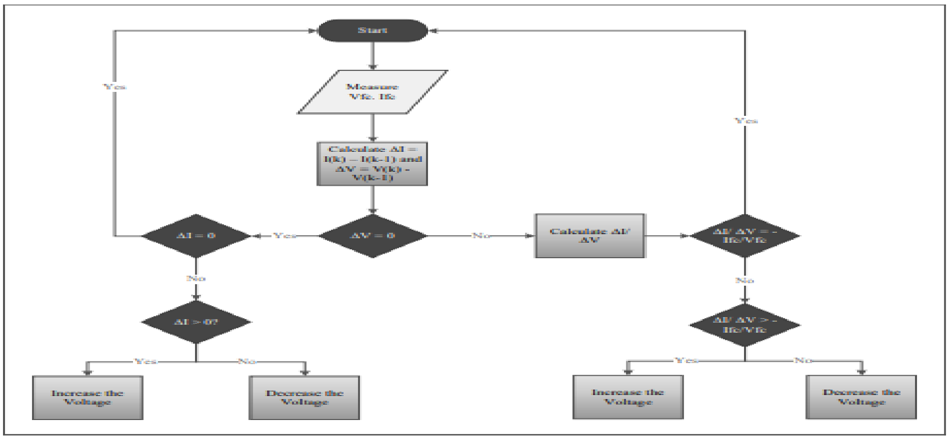

Figure 7: INC algorithm for the Fuel Cell

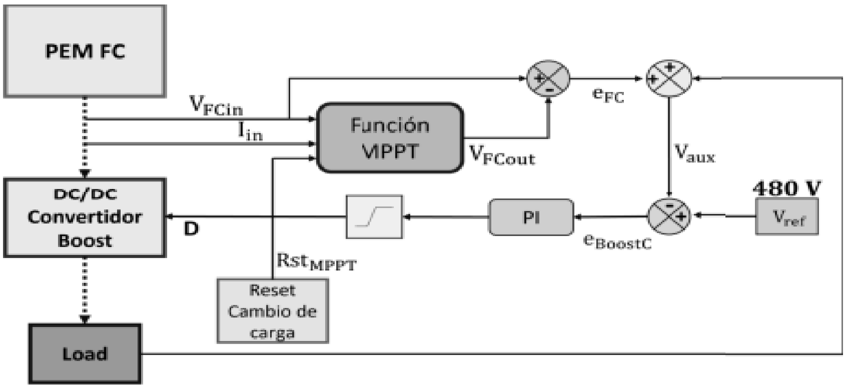

Figure 8: Control system block diagram

Figure 8 presents the controller between the FC and the DC-DC converter. The output voltage and current of the FC serve as the input variables for the P&O and IC controllers. The algorithms were programmed into a MATLAB function in which at each time step, an error in the FC is calculated (e_{FC}), through the difference between the input and output voltage $e_{FC} = V_{FCin} - V_{FCout}$. e_{FC} is then added to the output voltage of the converter to produce an auxiliary voltage (V_{aux}). This result is compared with the reference voltage (V_{ref}), generating an error related to the converter $e_{BoostC} = V_{ref} - V_{aux}$. The value of e_{BoostC} was then fed into the Proportional-Integral (PI) controller to produce the converter's duty cycle.

III. SIMULATIONS AND RESULTS

A comparative analysis was conducted to evaluate the performance of two MPPT control techniques (P&O and IC) for an FCBEV as shown in Figure 9. The developed control strategy focused on the FC-DC Boost Converter subsystem to regulate the DC bus voltage at 480 V under driving profile.

3.1 Using P&O Algorithm

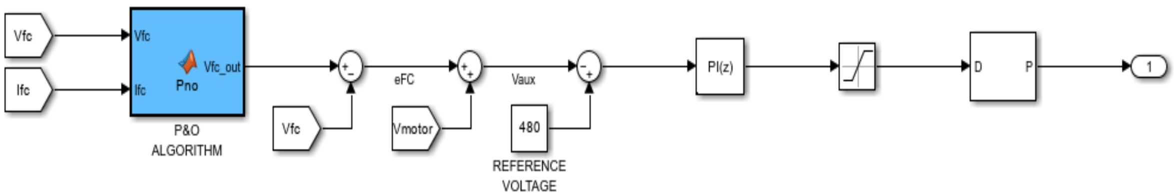

Figure 9: Controlling simulation diagram of P&O technique'

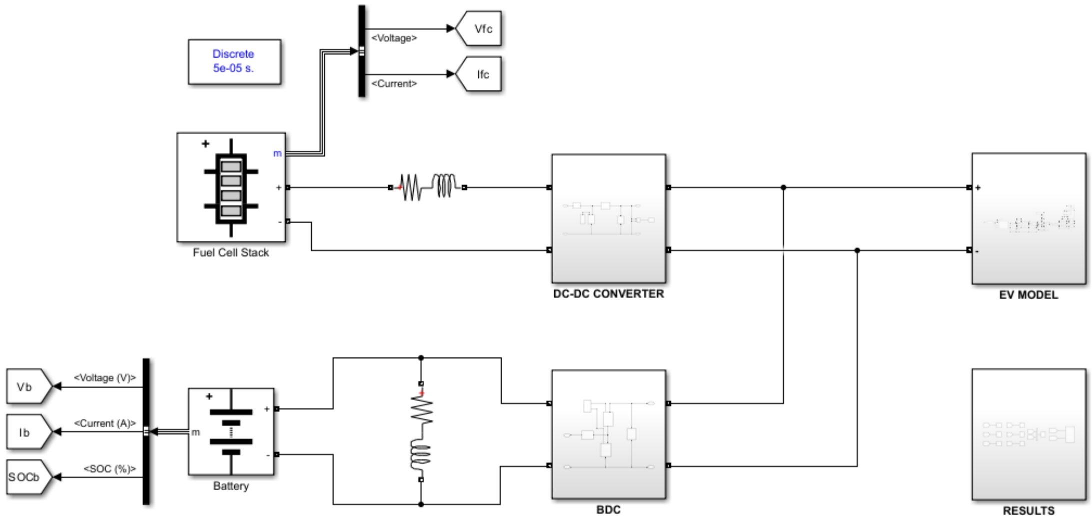

Figure 10: Simulation diagram of proposed system

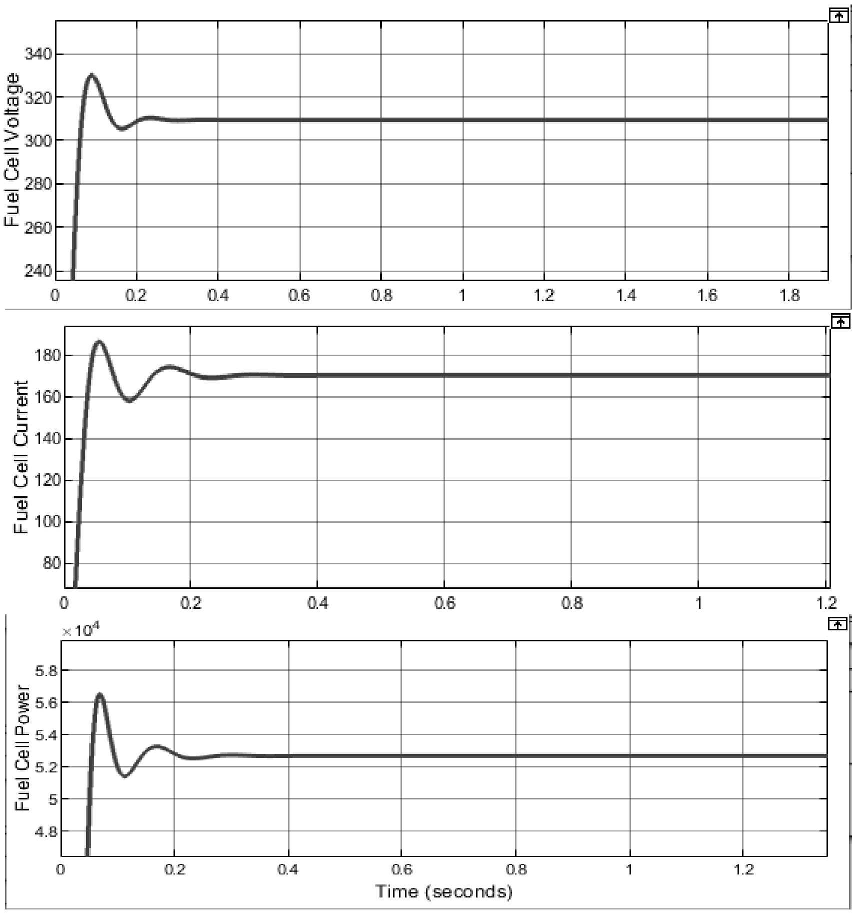

Figure 11 : Fuel Cell Voltage, Current & Power

The Figure 10 shows the Simulation diagram of proposed and Figure 11 shows the dynamic response of the fuel cell in terms of output voltage, current, and power under the proposed MPPT control strategy. Initially, all three parameters exhibit a small overshoot due to the startup transient of the fuel cell and boost converter. The fuel cell voltage settles at approximately 310 V, while the output current stabilizes around 170 A within 0.3 s. Similarly, the output power converges to nearly 52.5 kW after a brief transient period.

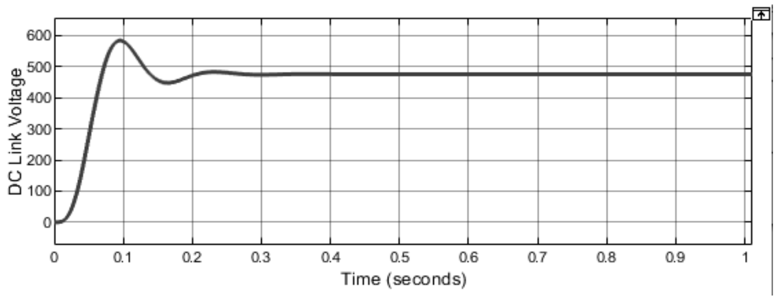

Figure 12: DC Link Voltage using P&O technique

Figure 12 shows the DC-link voltage response of the proposed fuel cell–battery hybrid electric vehicle system. During startup, the DC-link voltage rises rapidly and exhibits a small overshoot of approximately 580 V before settling.

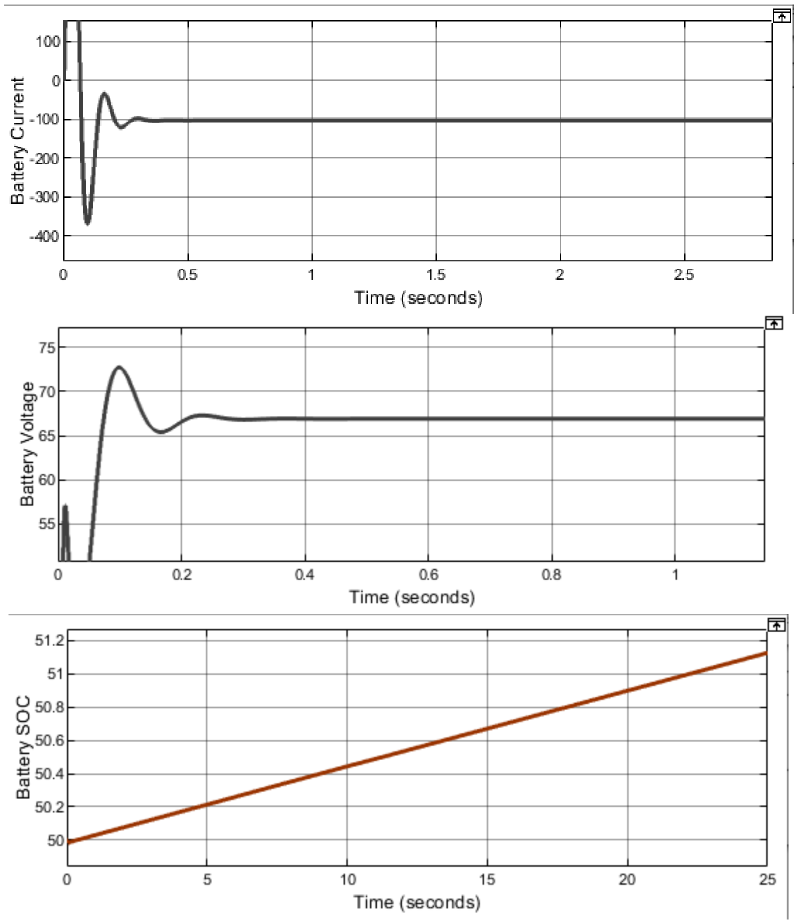

Figure 13:Battery Performance Characteristics

Figure 13 illustrates the battery performance in terms of current, voltage, and State of Charge (SOC) during the operation of the proposed fuel cell–battery hybrid electric vehicle. Initially, the battery current exhibits a transient response with a peak charging/discharging current before settling at approximately −100 A, indicating stable battery operation after the startup period. The battery voltage shows a small overshoot of about 73 V and gradually stabilizes at nearly 67 V within 0.3 s, demonstrating effective voltage regulation by the bidirectional DC–DC converter. The battery SOC increases gradually from 50% to approximately 51.2% over the simulation period, confirming that the battery is being charged while supporting the fuel cell system. The smooth increase in SOC without sudden fluctuations indicates proper energy management and balanced power sharing between the fuel cell and the battery. The smooth increase in SOC without sudden fluctuations indicates proper energy management and balanced power sharing between the fuel cell and the battery. Overall, the results demonstrate that the proposed control strategy effectively regulates battery current and voltage while maintaining a stable charging process.

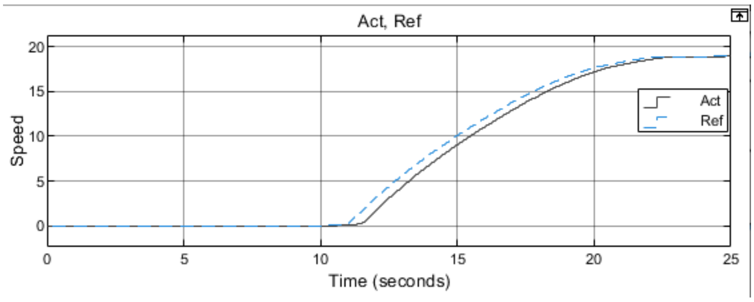

Figure 14: Actual & Reference Speed

Figure 14 shows the comparison between the reference speed and the actual speed of the electric vehicle. The actual speed closely follows the reference speed with a small delay during the acceleration period.

3.2 Using INC Algorithm

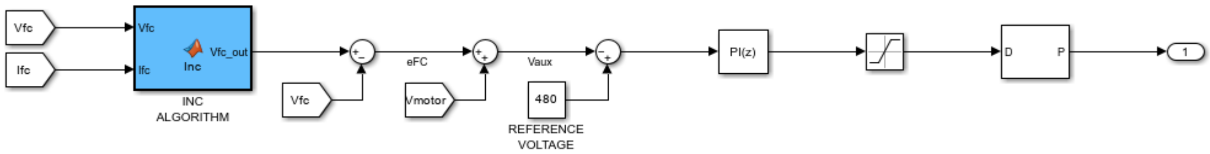

Figure 15: Controlling simulation diagram of INC technique

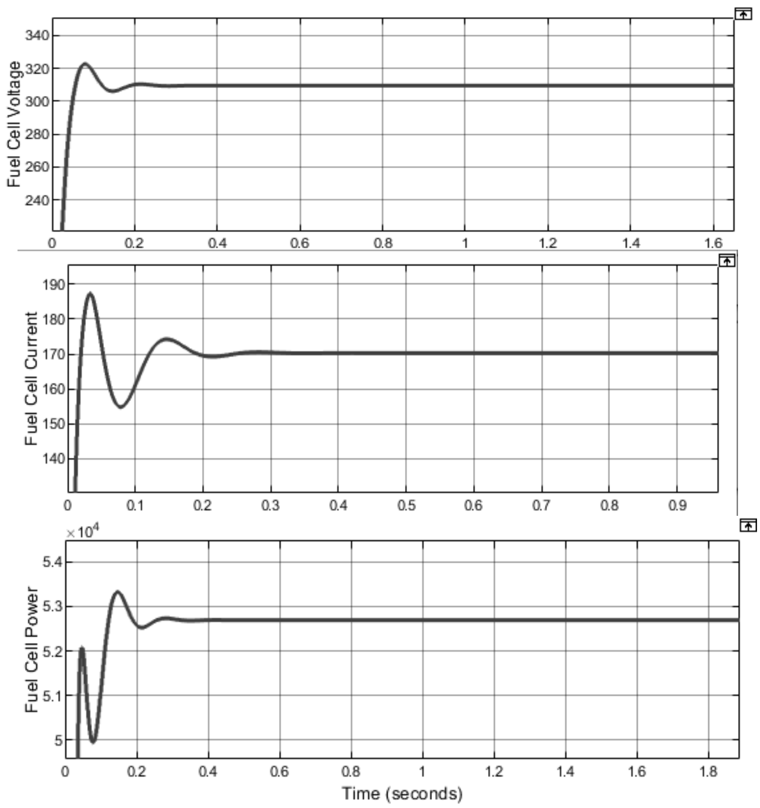

Figure 16:Fuel Cell Voltage, Current & Power

The Figure 15 displays Controlling simulation diagram of INC technique and the Figure 16illustrates the dynamic response of the fuel cell in terms of output voltage, current, and power under the proposed MPPT control strategy. During startup, the fuel cell voltage, current, and power exhibit small transient overshoots due to the converter initialization and controller action. The output voltage settles at approximately 310 V, while the fuel cell current stabilizes around 170 A within 0.3 s.

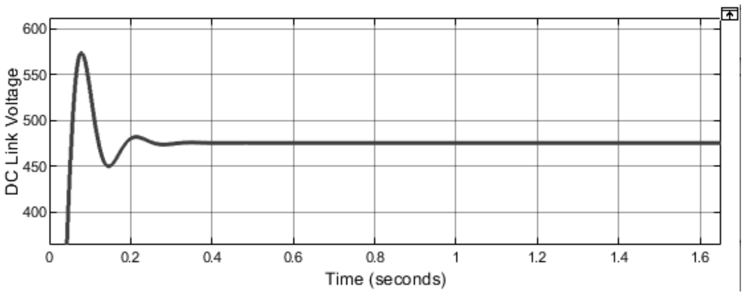

Figure 17: DC Link Voltage

Figure 17 shows the DC-link voltage response of the proposed fuel cell–battery hybrid electric vehicle under MPPT control. During startup, the DC-link voltage rises rapidly and exhibits a peak overshoot of approximately 575 V before decreasing toward the reference value.

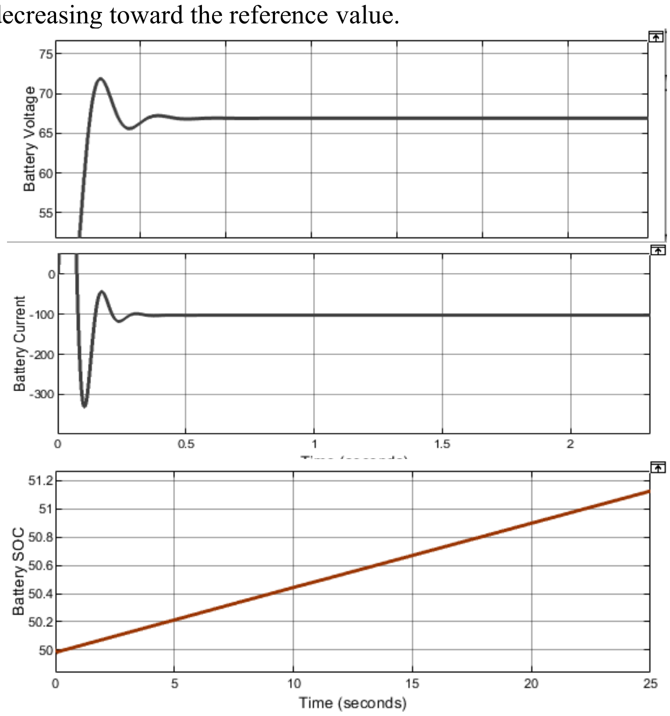

Figure 18: Battery Voltage, Current & SOC

Figure 18 illustrates the battery performance in terms of current, voltage, and State of Charge (SOC) under the proposed MPPT-based control strategy. During the startup period, the battery current exhibits a transient response with an initial peak charging/discharging current before settling to approximately −100 A, indicating stable battery operation. The battery voltage experiences a small overshoot during the transient period and stabilizes at around 67 V within 0.3s, demonstrating effective voltage regulation by the bidirectional DC–DC converter.

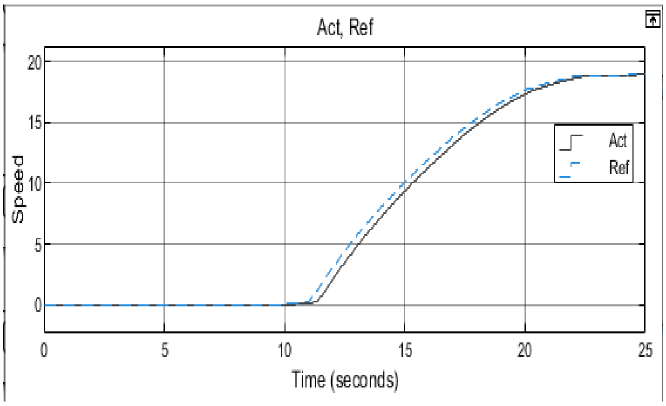

Figure 19: Actual & Reference Speed

By using Incremental Conductance algorithm, we can observe that there is a reduction of rise in peak as well as in actual speed which is shown in Fig19.

3.3 Using P&O Algorithm (Implementing GAO)

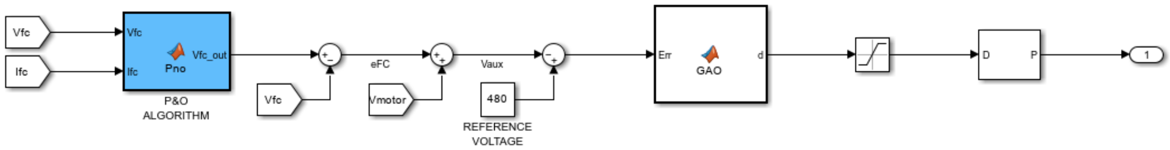

Figure 20: Controlling simulation diagram of P&O technique using GAO

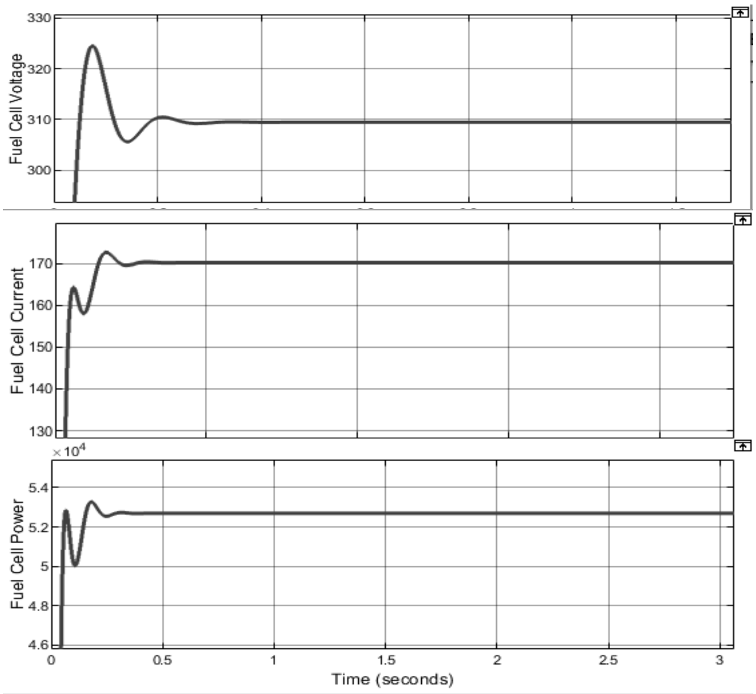

Figure 21: Fuel Cell Voltage, Current & Power

The fuel cell voltage, current, and power responses demonstrate in Figure 21. The dynamic performance of the proposed INC-GAO controller. Initially, all three parameters exhibit a small overshoot and oscillatory behaviour due to the rapid tracking of the optimal operating point. The fuel cell voltage rises quickly and settles at approximately 310 V within 0.3 s, indicating fast voltage regulation. Similarly, the fuel cell current stabilizes around 170 A after a brief transient response. The control simulation diagram of P&O technique using GAO shown in Figure 20

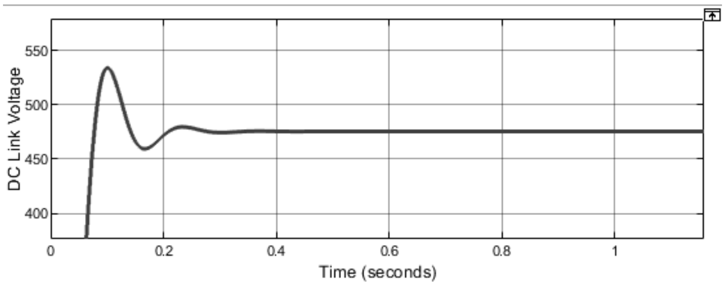

Figure 22: DC Link Voltage

The Figure 22 shows the DC link voltage response of the system using the Perturb and Observe (P&O) algorithm optimized with the Grasshopper Optimization Algorithm (GOA). At the start, the DC link voltage rises rapidly and reaches a peak of about 530 V, indicating a temporary overshoot during the transient response. It then decreases below the reference value and exhibits small oscillations as the controller adjusts the operating point. After approximately 0.3 seconds, the voltage settles at around 475 V with negligible fluctuations, demonstrating good damping and stability. This response indicates that the P&O-GOA approach provides fast convergence, reduced steady-state oscillations, and effective regulation of the DC link voltage.

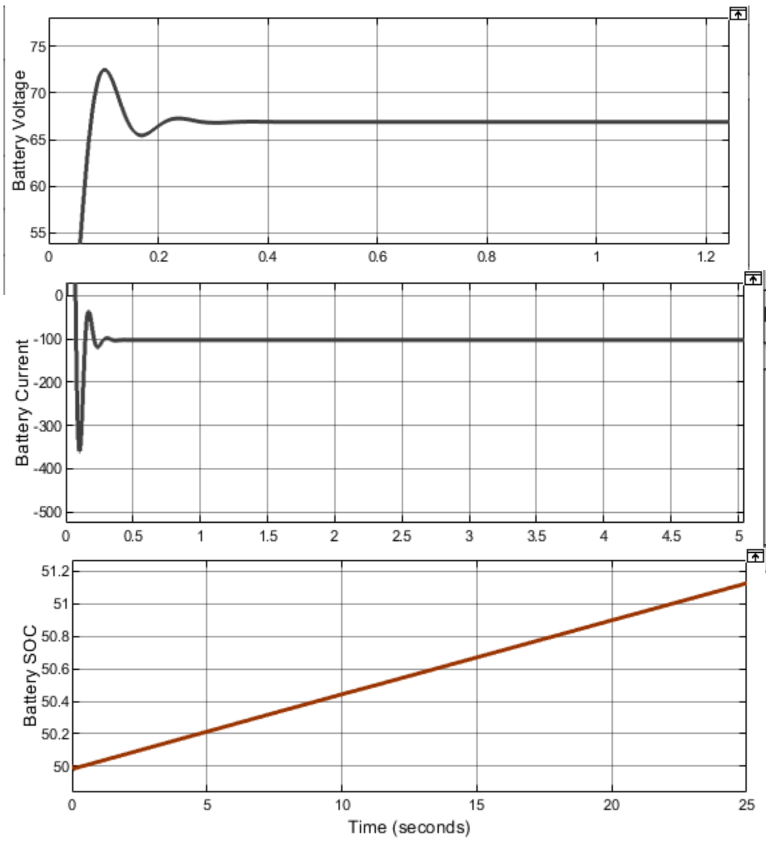

Figure 23: Battery Voltage, Current & SOC

The Figure 23 shows that the battery voltage rises rapidly with a small overshoot before settling at approximately 67 V within 0.3 seconds. This demonstrates that the P&O-GOA controller provides fast, stable, and well-damped voltage regulation. The battery current exhibits an initial transient before stabilizing at approximately −100 A within 0.4 seconds.

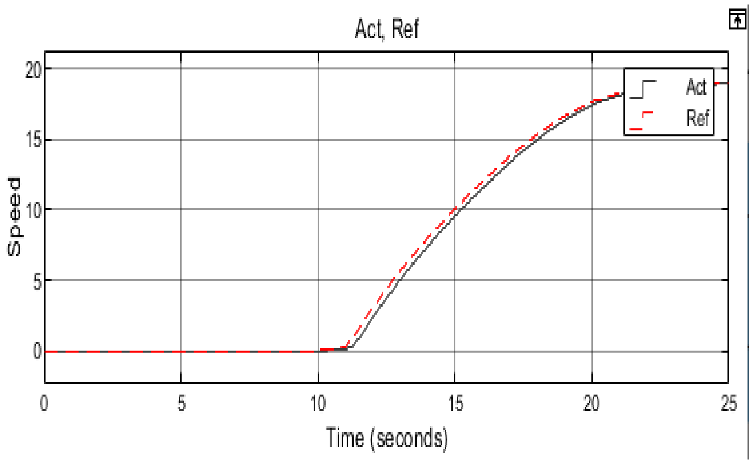

Figure 24: Actual & Reference Speed

The P&O-GAO controller accurately tracks the reference speed with only a small transient error after the speed command is applied at around 11 sis shown in Figure 24. The actual speed follows the reference smoothly with negligible overshoot and minimal oscillations.

3.4 Using INC Algorithm (Implementing GAO)

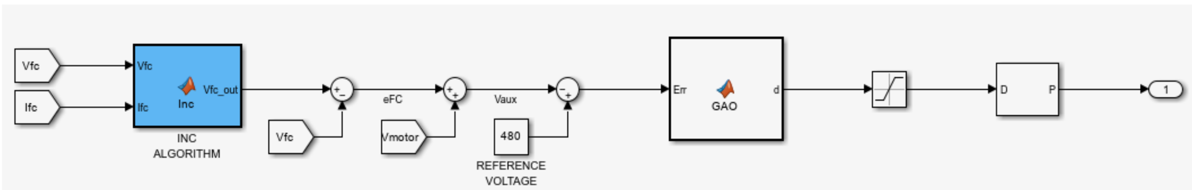

Figure 25: Controlling simulation diagram of P&O technique using GAO

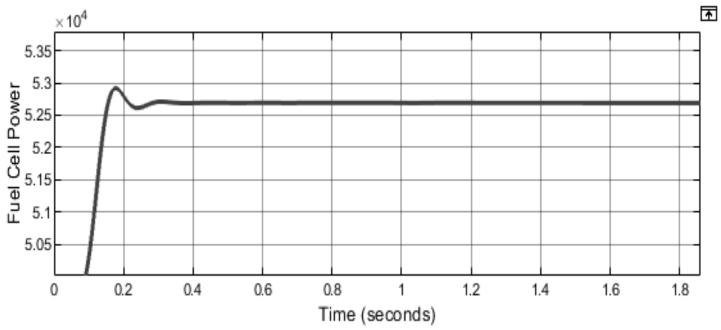

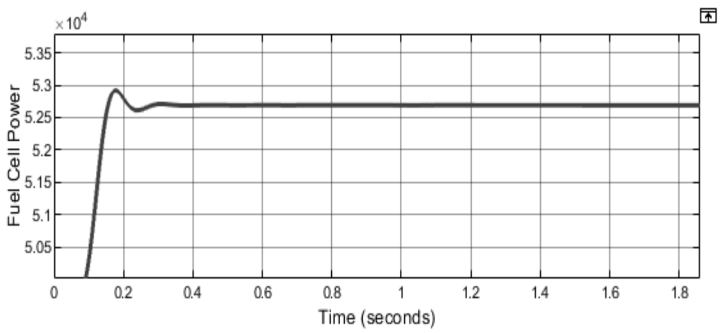

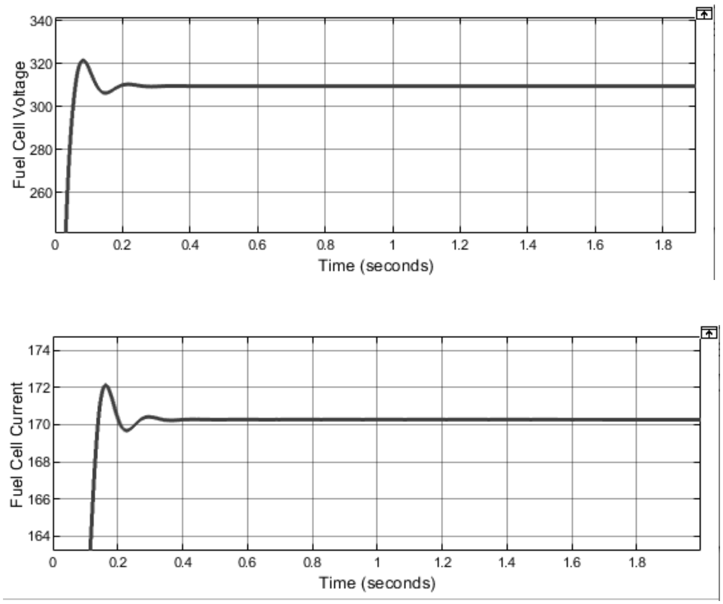

Figure 26: Fuel Cell Voltage, Current & Power

The Figure 26 shows that the fuel cell voltage exhibits a small transient overshoot during startup before settling at approximately 310 V. The oscillations decay rapidly, indicating a well-damped response. This demonstrates stable voltage regulation achieved using the P&O-GAO controller. The fuel cell current initially overshoots slightly and then settles quickly at approximately 170 A.

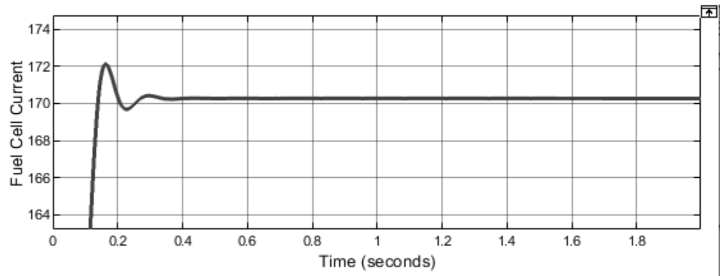

Figure 27: DC Link Voltage

The Figure 27 shows that the DC-link voltage falls from 520 V to 420 V over 1.6 seconds. This is likely a test of an incremental conductance MPPT algorithm combined with an adaptive optimisation (GAO), showing how the DC-link behaves under a changing power condition.

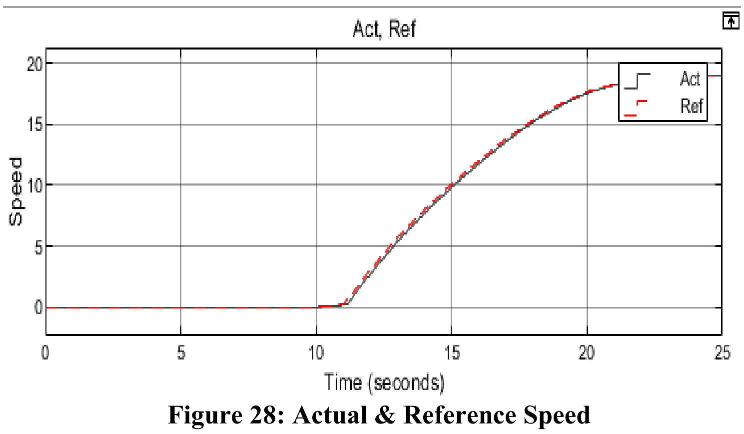

Figure 28: Actual & Reference Speed

The Figure 28shows graph plots Actual Speed (Act) and Reference Speed (Ref) against Time (seconds) to evaluate the speed tracking performance of the system. The Ref line represents the desired or commanded speed profile, while the Act line shows the measured response of the motor or drive.

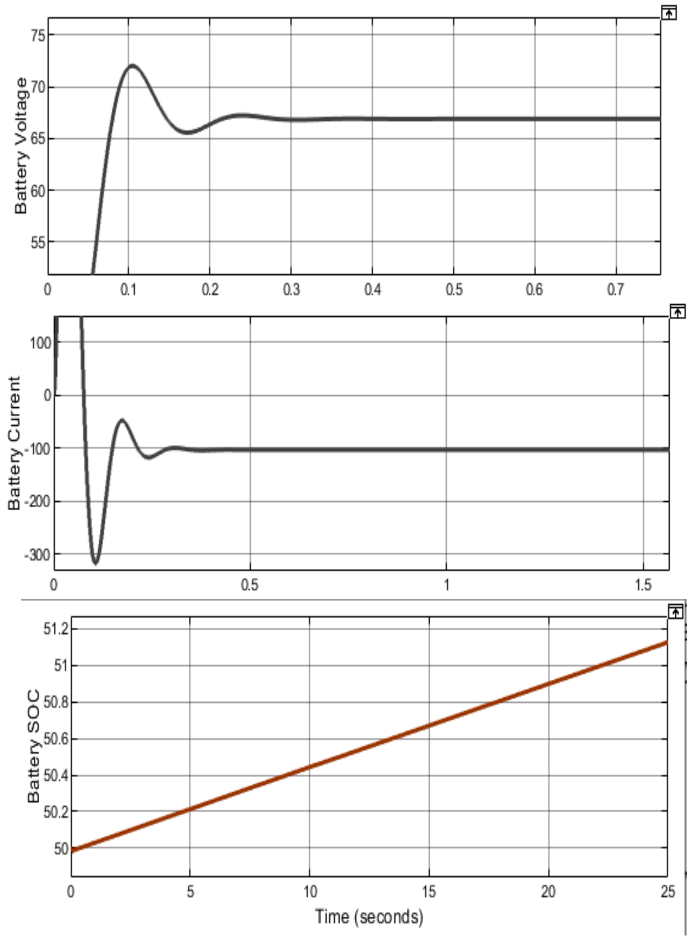

Figure 29: Battery Voltage, Current & SOC

From Figure 29 shows the battery voltage starts at 52.0 V and rises rapidly to 67.0 V within the first 0.18 seconds, after which it remains stable at 67.0 V for the entire remaining duration. Simultaneously, the battery current is maintained at a constant 100 A from t=0 to t=1.50 seconds, indicating a steady charge rate.

3.5 Comparison Table

Table 4: Fuel cell comparison

Component	Parameter	Metrics	PI		GAO	
			P&O	INC	P&O	INC
Fuel Cell	Voltage (V_{fc})	Settling Time (s)	0.1240	0.1040	0.1011	0.1051
		Peak	330.159	322.593	324.540	321.448
		Overshoot (%)	6.684	4.244	4.869	3.874
		Ripple (%)	0.072	0.074	0.075	0.072
	Current (I_{fc})	Settling Time (s)	0.1778	0.1575	0.1301	0.1254
		Peak	186.684	187.361	172.739	172.134

		Overshoot (%)	9.643	10.040	1.453	1.097
		Ripple (%)	0.151	0.155	0.134	0.131

Table 4 presents the comparative performance of the conventional PI controller and the GAO-based controller employing the P&O MPPT technique for the fuel cell's voltage and current parameters. The GAO controller demonstrates superior dynamic performance by reducing the settling time, peak value, and overshoot for both parameters. A significant improvement is observed in the current response, where the overshoot is reduced by 84.93%, while the voltage response exhibits faster stabilization with only a negligible variation in ripple. These results confirm the effectiveness of the GAO controller in enhancing the transient and steady-state performance of the system.

Table 5: DC Link voltage comparison

Component	**Parameter**	**Metrics**	**PI**		**GAO**	
			P&O	**INC**	**P&O**	**INC**
DC-Link	**Voltage (Vdc)**	**Settling Time (s)**	0.1933	0.1738	0.1879	0.1786
		Peak	583.508	573.574	533.959	517.648
		Overshoot (%)	22.744	20.655	12.322	8.890
		Ripple (%)	0.347	0.350	0.308	0.297

Table 5 presents the comparative performance of the PI and GAO controllers for DC-link voltage regulation under the P&O and INC-MPPT techniques. The GAO controller exhibits improved transient and steady-state characteristics by reducing the settling time, peak voltage, overshoot, and ripple compared to the conventional PI controller. Among all the evaluated cases, the GAO with INC-MPPT achieves the best performance, exhibiting the lowest peak voltage (517.648 V), overshoot (8.890%), and ripple (0.297%).

Table 6 : Speed comparison

Component	**Parameter**	**Metrics**	**PI**		**GAO**	
			P&O	**INC**	**P&O**	**INC**
Motor	**Speed**	**Settling Time**	21.9931	21.8489	21.7431	21.6416

Table 6 compares the motor speed response of the PI and GAO controllers under the P&O and INC-MPPT techniques based on the settling time. The GAO controller consistently achieves a faster settling response than the conventional PI controller for both MPPT methods. Among the evaluated cases, the GAO–INC configuration provides the minimum settling time of 21.6416 s, indicating the fastest speed stabilization. These results demonstrate that the GAO controller enhances the dynamic response of the motor drive and improves the overall transient performance of the proposed system.

IV. CONCLUSION

This work presented a comparative performance evaluation of PI and Gazelle Optimization Algorithm (GAO) based controllers integrated with Perturb and Observe (P&O) and Incremental Conductance (INC) MPPT techniques for a fuel cell-powered electric drive system. The controller performance was analyzed using the transient and steady-state responses of the fuel cell voltage, fuel cell current, DC-link voltage, and motor speed.

The simulation results demonstrate that the GAO-based controller consistently outperforms the conventional PI controller in all key performance indices. For the fuel cell voltage, the GAO controller reduced the settling time to 0.1011 s (P&O) and 0.1051 s (INC), while limiting the voltage overshoot to 4.869% and 3.874%, respectively. In the fuel cell current response, the proposed controller achieved a significant reduction in overshoot from 9.643% to 1.453% with P&O and from 10.040% to 1.097% with INC, corresponding to improvements of approximately 84.93% and 89.07%, respectively.

Similarly, the DC-link voltage regulation was considerably enhanced, where the GAO–INC configuration achieved the lowest peak voltage (517.648 V), minimum overshoot (8.890%), and lowest ripple (0.297%), ensuring improved voltage stability. The motor speed response also exhibited faster stabilization, with the GAO–INC controller providing the minimum settling time of 21.6416 s.

Among the four controller-MPPT combinations investigated, the GAO controller combined with the Incremental Conductance (INC) MPPT algorithm delivered the best overall performance. It provided faster transient response, reduced overshoot, lower ripple, improved voltage regulation, and enhanced speed stability compared to the conventional PI controller. These improvements reduce electrical and mechanical stresses on the system components, improve energy utilization, and enhance the reliability of the fuel cell-powered drive.

Overall, the results confirm that integrating the Gazelle Optimization Algorithm with the INC-MPPT technique significantly improves the dynamic and steady-state performance of the proposed fuel cell-based electric drive system. The proposed control strategy is therefore well suited for practical applications such as fuel cell electric vehicles (FCEVs), hybrid electric vehicles (HEVs), industrial motor drives, renewable energy systems, battery-assisted fuel cell systems, and smart microgrid applications, where high efficiency, rapid response, and stable operation are essential.

REFERENCES

[1] D. F. Pereira, F. D. C. Lopes, and E. H. Watanabe, "Nonlinear Model Predictive Control for the Energy Management of Fuel Cell Hybrid Electric Vehicles in Real Time," IEEE Transactions on Industrial Electronics, vol. 68, no. 4, pp. 3213–3223, Apr. 2021, doi: 10.1109/TIE.2020.2979528.

[2] H. Lee and S. W. Cha, "Energy Management Strategy of Fuel Cell Electric Vehicles Using Model-Based Reinforcement Learning with Data-Driven Model Update," IEEE Access, vol. 9, pp. 59244–59254, 2021, doi: 10.1109/ACCESS.2021.3072903.

[3] A. Ferrara and C. Hametner, "Impact of Energy Management Strategies on Hydrogen Consumption and Start-Up/Shut-Down Cycles in Fuel Cell-Ultra-capacitor-Battery Vehicles," IEEE Trans Veh Technol, vol. 71, no. 6, pp. 5692–5703, Jun. 2022, doi: 10.1109/TVT.2021.3127582.

[4] S. George and T. Rajeev, "Fuzzy Based Hybrid Control Topology for Fuel Cell and Battery Powered EV," 2022 IEEE 2nd International Conference on Sustainable Energy and Future Electric Transportation, SeFeT 2022, 2022, doi: 10.1109/SEFET55524.2022.9909199.

[5] M. Pathmanathan, S. Semsar, C. Viana, and P. W. Lehn, "Power Sharing Control Algorithm for Direct Integration of Fuel Cells in a Dual-Inverter Electric Vehicle Drivetrain," IEEE Transactions on Transportation Electrification, vol. 8, no. 2, pp. 2490–2500, Jun. 2022, doi: 10.1109/TTE.2022.3143092.

[6] M. Moghadari, M. Kandidayeni, L. Boulon, and H. Chaoui, "Operating Cost Comparison of a Single-Stack and a Multi-Stack Hybrid Fuel Cell Vehicle Through an Online Hierarchical Strategy," IEEE Trans Veh Technol, vol. 72, no. 1, pp. 267–279, Jan. 2023, doi: 10.1109/TVT.2022.3205879.

[7] A. Haxhiu, A. Abdelhakim, S. Kanerva, and J. Bogen, "Electric Power Integration Schemes of the Hybrid Fuel Cells and Batteries-Fed Marine Vessels - An Overview," IEEE Transactions on Transportation Electrification, vol. 8, no. 2, pp. 1885–1905, Jun. 2022, doi: 10.1109/TTE.2021.3126100.

[8] A. Meshginqalam and J. Bauman, "Integrated Convex Speed Planning and Energy Management for Autonomous Fuel Cell Hybrid Electric Vehicles," IEEE Transactions on Transportation Electrification, vol. 9, no. 1, pp. 1072–1086, Mar. 2023, doi: 10.1109/TTE.2022.3200013.

[9] S. K. Das and J. Kim, "Evaluation of Power Sharing Mechanism of a PEM Fuel Cell-Battery Powered Electric Vehicle," 2023 4th International Conference on Clean and Green Energy Engineering, CGEE 2023, pp. 112–118, 2023, doi: 10.1109/CGEE59468.2023.10351891.

[10] S. George, N. Sehgal, K. P. S. Rana, and V. Kumar, "A comprehensive review on modelling and maximum power point tracking of PEMFC," Cleaner Energy Systems, vol. 3, p. 100031, Dec. 2022, doi: 10.1016/J.CLES.2022.100031.

[11] F. Segura, F. J. Vivas, J. M. Andujar, and M. Martinez, "Hydrogen-powered refrigeration system for environmentally friendly transport and delivery in the food supply chain," Appl Energy, vol. 338, p. 120945, May 2023, doi: 10.1016/J.APENERGY.2023.120945.

[12] T. Hai, A. K. Alazzawi, J. Zhou, and H. Farajian, "Performance improvement of PEM fuel cell power system using fuzzy logic controller-based MPPT technique to extract the maximum power under various conditions", Int J Hydrogen Energy, vol. 48, no. 11, pp. 4430–4445, Feb. 2023, doi: 10.1016/J.IJHYDENE.2022.10.103.

[13] M. Derbeli, O. Barambones, M. Y. Silaa, and C. Napole, "Real-Time Implementation of a New MPPT Control Method for a DC-DC Boost Converter Used in a PEM Fuel Cell Power System," Actuators 2020, Vol. 9, Page 105, vol. 9, no. 4, p. 105, Oct. 2020, doi: 10.3390/ACT9040105.

[14] H. Rezk and A. Fathy, "Performance Improvement of PEM Fuel Cell Using Variable Step-Size Incremental Resistance MPPT Technique," Sustainability 2020, Vol. 12, Page 5601, vol. 12, no. 14, p. 5601, Jul. 2020, doi: 10.3390/SU12145601.